

Analysis of impact response and damage in laminated composite cylindrical shells undergoing large deformations

Surendra Kumar*

*CSIR Centre for Mathematical Modelling and Computer Simulation, NAL Belur Campus,
Bangalore-560037, India*

(Received April 29, 2008, Accepted January 28, 2010)

Abstract. The impact behaviour and the impact-induced damage in laminated composite cylindrical shell subjected to transverse impact by a foreign object are studied using three-dimensional non-linear transient dynamic finite element formulation. A layered version of 20 noded hexahedral element incorporating geometrical non-linearity is developed based on total Lagrangian approach. Non-linear system of equations resulting from non-linear strain displacement relation and non-linear contact loading are solved using Newton-Raphson incremental-iterative method. Some example problems of graphite/epoxy cylindrical shell panels are considered with variation of impactor and laminate parameters and influence of geometrical non-linear effect on the impact response and the resulting damage is investigated.

Keywords: finite element analysis; large deformation; 20 noded layered hexahedral element; polymer matrix composites; laminated shell; impact.

1. Introduction

One of the important considerations in the design of fibre-reinforced plastic laminated composite structure is the resistance of the damage caused by low velocity non-penetrating impact. Accordingly, many experimental and analytical investigations have been reported towards understanding impact response and predicting impact-induced damage in these laminates. A number of researchers have deployed the 2-D and 3-D finite element method for the solution of impact on laminated composites. Abrate (1994) reviewed most of the earlier work in this field. In spite of extensive literature available on the subject, there is continuing interest by researchers because several issues pertaining to complicated impact damage phenomena and effects of several parameters are involved. Some of the recent studies in this field include damage analysis of curved structures, large deformation analysis and inelastic behavior of matrix material.

Most of the earlier impact problems for laminated plates and shells have been formulated using small deflection theory and damage analysis has been mainly confined to laminated plates. Ambur *et al.* (1995) have concluded that non-linear effects can be significant for thin and moderately thick laminated composite plates subjected to low-velocity impact. Chandrashekhara and Schroeder

*Ph.D., E-mail: surendra@cmmacs.ernet.in

(1995) have studied impact response of laminated curved shells using finite element formulation based on Sander's shell theory considering geometric non-linearity in the sense of von Karman strains. However, impact damage was not investigated in their study. Ganapathy and Rao (1998) used 4-noded 48 d.o.f shell element based on Kirchhoff-Love thin shell theory in non-linear finite element analysis of cylindrical/spherical shell panels. The authors predicted matrix cracking failure by applying the general Tsai-Wu failure criterion for composite materials. Although geometrical non-linearity was included, the study assumes that low velocity impact force and deformation can be simulated by static model and hence does not compute impact response as a function of time. Krishnamurthy *et al.* (2001) used 9-noded shell element accounting for large deformation in their parametric studies of impact on laminated cylindrical composite shells. The shell element was based on Mindlin-Reissner assumptions regarding transverse shear deformations and assumed parabolic shear stress distribution across the thickness. In another paper (Krishnamurthy *et al.* 2003), the authors extended their work on impact response of a laminated composite cylindrical shell as well as a full cylinder by incorporating the classical Fourier series method into the finite element formulation and also predicted impact-induced damage using the semi-empirical damage prediction model of Choi and Chang (1992). According to the authors, the Fourier series method, which gives information regarding the natural frequencies of vibration of the impacted structure, provided a proper basis for adopting the appropriate size of the analysis time step. However, the paper doesn't address non-linear effects. Hou *et al.* (2000) provided details of the implementation of improved failure criteria for laminated composite structures under impact loading. Out-of-plane stresses were taken into consideration for damage initiation. It was suggested, for the first time, that delamination is constrained by through-thickness compression stress. In another paper (Hou *et al.* 2001), the authors improved the delamination criterion by taking into consideration both the interlaminar shear and through-thickness compression stresses and verified it by experimental results for low-velocity impact. Cho and Zhao (2002) investigated the effects of geometrical and material factors on the mechanical behavior of composite laminates under low velocity impact and compared results obtained by 2-D and 3-D finite element methods. In another paper (Zhao and Cho 2004), the authors investigated impact behavior in composite shells by a low-velocity projectile using 3-D eight-noded brick element formulation based on linear elasticity theory. They analyzed damage using Tsai-Wu quadratic failure criterion and delamination formula suggested by Hou *et al.* (2000). They validated the numerical results with experimental result by Choi and Chang (1992) for laminated plate and also concluded that damage propagation in composite shell takes place much differently from that in composite plate. Her and Liang (2004) have studied the transient response of impact in cylindrical and spherical shells using 3-D finite element formulation. Impact-induced damages (matrix cracking and delamination) were predicted using failure criteria suggested by Choi and Chang (1992). However, large deformation effect was not included in their analysis. The investigations by Gning *et al.* (2005) involved the identification and modeling of damage initiation and development in glass-reinforced epoxy composite cylinders subjected to drop weight impact. Delamination was characterized using an energy balance model under the assumption that the loss in energy of the impactor during a drop weight impact is entirely used to create delaminations. Zhu *et al.* (2006) incorporated effects of strain rate dependency and inelastic behavior of matrix material for analyzing the mechanical response of laminated shell. The study was, however, concentrated on transient response of laminated shell subjected to suddenly applied static loading uniformly distributed over the bottom surface of the panel and also didn't consider damage phenomena. In the paper by Kumar *et al.* (2007), the authors have carried out parametric studies on impact response

and damage in curved composite laminates using 3D eight noded layered brick element and investigated effect of material degradation. However, formulation was based on linear elasticity theory.

In the present paper, a non-linear three-dimensional transient dynamic finite element analysis is carried out to predict impact-induced damage in curved composite laminate subjected to transverse impact by a metallic impactor. A layered version of twenty noded isoparametric hexahedral element incorporating geometrical non-linearity is developed based on total Lagrangian approach and the generalized Green's strain tensor is used in the strain-displacement relationships. In author's knowledge, the use of layered 20 noded brick element as such or in combination with geometrical non-linearity has not been reported in open literature. The layered version of this element is different from the isotropic element in the sense that it can contain multiple plies inside it and accounts for changes in material properties and orientation of the plies inside the element. For computational efficiency, 14 point integration formula is used instead of standard $3 \times 3 \times 3$ formula for numerical integration of element matrices. The non-linear system of equations resulting from large deformation formulation and non-linear contact law are simultaneously solved iteratively using Newton-Raphson method. Example problems of graphite/epoxy cylindrical shell panels with parametric variations are considered and influence of geometrical non-linearity on the impact response and resulting damage is discussed.

2. Finite element methodology

2.1 Non-linear equilibrium equations

Using the principle of virtual work, the finite element equation of equilibrium after including the inertia forces at time t_{n+1} can be given as (Zienkiewicz and Taylor 1993)

$$\{\Psi_{n+1}\} = \int_V [B]^T \{\sigma_{n+1}\} dV + \int_V [N]^T \rho \{\ddot{u}_{n+1}\} dV - \{F_{n+1}\} \quad (1)$$

where $\{\Psi_{n+1}\}$ is residual or out-of-balance force vector, $[B]$ strain-displacement matrix, $\{\sigma_{n+1}\}$ stress vector at any point, $[N]$ shape function matrix, ρ mass density, $\{\ddot{u}_{n+1}\}$ acceleration vector at any point and $\{F_{n+1}\}$ is load vector which consists of contact force between impactor and shell.

In the large displacement problem

$$[B] = [B_L] + [B_{NL}] \quad \text{and}$$

$$\{\sigma_{n+1}\} = [C] \left[[B_L] + \frac{1}{2} [B_{NL}] \right] \{U_{n+1}\} = [C] [\bar{B}] \{U_{n+1}\} \quad (2)$$

where $[B_L]$ is the contribution from the linear part of the Green's strain and $\frac{1}{2}[B_{NL}]$ is the contribution from the quadratic part of the Green's strain and is a linear function of the element nodal displacements $\{U_{n+1}\}$. $[C]$ is the material property matrix relating the strains to the stresses in global coordinate system.

In Eq. (1)

$$\{\ddot{u}_{n+1}\} = [N] \{\ddot{U}_{n+1}\} \quad (3)$$

Using Newmark implicit time integration method with constant average acceleration ($\alpha=0.5$ and $\beta = 0.25$), the nodal acceleration vectors $\{\ddot{U}_{n+1}\}$ can be expressed in terms of nodal displacements $\{U_{n+1}\}$ as follows

$$\{\ddot{U}_{n+1}\} = \frac{1}{\beta(\Delta t)^2}\{U_{n+1}\} - \left(\frac{1}{\beta(\Delta t)^2}\{U_n\} + \frac{1}{\beta(\Delta t)}\{\dot{U}_n\} + \frac{1-2\beta}{2\beta}\{\ddot{U}_n\} \right) \quad (4)$$

Eqs. (3) and (4) can be put into Eq. (1) to form

$$\{\Psi_{n+1}\} = \int_V [B]^T \{\sigma_{n+1}\} dV + \frac{1}{\beta(\Delta t)^2} \left(\int_V [N]^T \rho_{n+1} [N] dV \right) \{U_{n+1}\} - \{F_{n+1}^M\} - \{F_{n+1}\} \quad (5)$$

In Eq. (5), $\{F_{n+1}^M\}$ can be referred to as load vector due to inertia term at time t_{n+1} and is given as

$$\{F_{n+1}^M\} = [M] \left(\frac{1}{\beta(\Delta t)^2}\{U_n\} + \frac{1}{\beta(\Delta t)}\{\dot{U}_n\} + \frac{1-2\beta}{2\beta}\{\ddot{U}_n\} \right) \quad (6)$$

In Eq. (6), $[M] = \int_V [N]^T \rho_{n+1} [N] dV$ is the mass matrix.

The solution of non-linear Eq. (5) is achieved iteratively using Newton-Raphson scheme. It is, therefore, necessary to find relation between $\{d\Psi_{n+1}\}$ and $\{dU_{n+1}\}$. If Eq. (5) is differentiated, we have

$$[K_{T(n+1)}] \{dU_{n+1}\} = \{d\Psi_{n+1}\} \quad (7)$$

where tangent stiffness matrix $[K_{T(n+1)}]$ is

$$[K_{T(n+1)}] = \int_V [B]^T [C] [B] dV + \int_V [G]^T [S_{n+1}] [G] dV + \frac{1}{\beta(\Delta t)^2} \left(\int_V [N]^T \rho_{n+1} [N] dV \right) \quad (8)$$

In Eq. (8), $[G]$ is matrix of shape function derivatives and $[S]$ is a matrix of stress array. For the present 3D element, $[S]$ is given as

$$[S] = \begin{bmatrix} \sigma_x [I] & \tau_{xy} [I] & \tau_{xz} [I] \\ & \sigma_y [I] & \tau_{yz} [I] \\ sym. & & \sigma_z [I] \end{bmatrix},$$

where $[I]$ is an identity matrix of size 3×3 .

2.2 20-noded layered brick element

In the present analysis, three-dimensional 20-noded isoparametric layered brick element (Fig. 1) is developed to model the laminated structure. Element tangent stiffness matrix for this element is given as

$$[K_{T(n+1)}] = \int_{-1}^{+1} \int_{-1}^{+1} \int_{-1}^{+1} [B]^T [T]^T [\bar{C}] [T] [B] \det[J] d\xi d\eta d\zeta + \int_{-1}^{+1} \int_{-1}^{+1} \int_{-1}^{+1} [G]^T [S_{n+1}] [G] \det[J] d\xi d\eta d\zeta + \frac{1}{\beta(\Delta t)^2} \left(\int_{-1}^{+1} \int_{-1}^{+1} \int_{-1}^{+1} [N]^T \rho_{n+1} [N] \det[J] d\xi d\eta d\zeta \right) \quad (9)$$

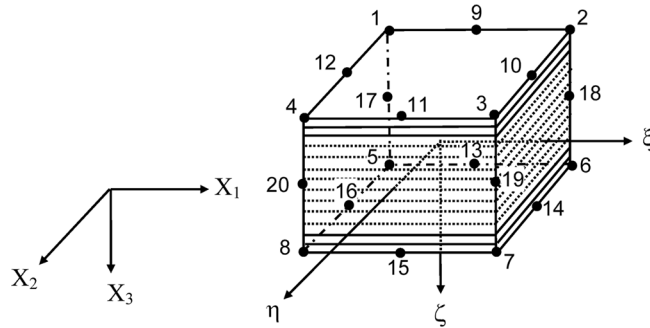


Fig. 1 Layered version of twenty-noded isoparametric brick element

In above equation, $[\bar{C}]$ is the material property matrix relating the strains within the ply to the stresses in ply coordinate system and $[T]$ is the transformation matrix relating the strains in the ply principal directions to those in the global reference axis. The material density ρ , the elasticity matrix $[\bar{C}]$, transformation matrix $[T]$ and $[S]$ matrix in Eq. (9) depend on the material properties and the orientations of the plies through the thickness of the element. This element formulation was implemented in our computer program in such a way that when the material properties and ply orientations are same through the thickness, numerical integrations of the equation using Gaussian quadrature is carried out at element level, otherwise it is accomplished from one ply-group to another ply-group through the element thickness.

2.3 Calculation of impact force

In order to solve Eq. (5), the contact force between impactor and laminated shell must be known. Although, the present formulation can simulate any type of complex contact conditions between impactor and laminate, the modified version of Hertzian contact law proposed by Yang and Sun (1982) is used in this study. This approach consists of determining the relationship between contact force F^c with the indentation depth α during loading and unloading.

For brevity, the contact force $(F_c)_{n+1}$ can be written in general form of contact law as

$$(F_c)_{n+1} = \phi(\alpha_{n+1}) = \phi(d_{n+1} - w_{n+1}) \tag{10}$$

where d_{n+1} is the displacement of the centre point of the impactor at $(n+1)$ th time-step. w_{n+1} is the displacement of mid-surface of the laminate at the impact point in the direction of impact. d_{n+1} is calculated by applying Newmark's method to equation of motion of impactor (Chandrashekhara and Schroeder 1995). The following expressions for velocity and displacement of the impactor are obtained

$$\begin{aligned} \dot{d}_{n+1} &= \dot{d}_n - \frac{1}{2} \frac{(F_c)_n + (F_c)_{n+1}}{m} \Delta t \\ d_{n+1} &= d_n + \dot{d}_n \Delta t - \frac{1}{4} \frac{(F_c)_n + (F_c)_{n+1}}{m} (\Delta t)^2 \end{aligned} \tag{11}$$

In a particular iteration $(i + 1)$ of $(n + 1)$ th time-step, the contact force can be expressed as

$$(F_c)_{n+1}^{i+1} = \phi \left(d_n + \dot{d}_n \Delta t - \frac{1}{4} \frac{(F_c)_n + (F_c)_{n+1}^{i+1}}{m} (\Delta t)^2 - w_{n+1}^t \right) \quad (12)$$

The $(F_c)_{n+1}^{i+1}$ is computed from the above equation using Newton-Raphson root finding algorithm.

2.4 Stress calculation

From the known displacements, the strains are calculated at reduced integration Gaussian points $2 \times 2 \times 2$ inside finite elements, since they have most precise values at these points. These strains are extrapolated at the vertex nodes of the element using trilinear extrapolation in the local coordinate system. Values for midside nodes are calculated as an average between values for two vertex nodal values. Then a global smoothing is performed for all nodes of the finite element model by averaging of contributions from the neighboring finite elements. Since the element may contain several plies of different orientations, the strains in each individual ply are calculated from element strains using interpolation procedure. The strains in each ply are then transformed in material axes system using standard formula for transformation of strains. Finally the stresses in each ply are obtained using the stress-strain relation for the ply in material axes system. Once the combined state of stress is known, appropriate failure criterion may be applied to predict the impact-induced damages within each ply. This procedure is repeated for each time step.

2.5 Impact damage analysis

Impact damage in laminated composite is a very complicated phenomenon and there are still no generally accepted analytical models that can accurately predict the damages. It is reported in previous study (Choi and Chang 1992) that intraply matrix cracking is the initial damage mode. Delamination initiates once the matrix crack reaches at the interfaces between the ply groups containing different fibre orientations after propagating throughout the thickness of the ply group that contained the cracked ply. This type of matrix crack is referred to as the "critical matrix crack". The authors (Choi and Chang 1992) proposed two failure criteria, critical matrix cracking criterion and impact-induced delamination criterion. They validated these damage models with experimental observations and also suggested some empirical constants.

The critical matrix cracking criterion for n th ply is given as

$$\left(\frac{{}^n \bar{\sigma}_y}{{}^n Y} \right)^2 + \left(\frac{{}^n \bar{\tau}_{yz}}{{}^n S_i} \right)^2 = e_m^2 \begin{cases} Y = Y_t, & \text{if } \bar{\sigma}_y \geq 0 \\ Y = Y_c, & \text{if } \bar{\sigma}_y < 0 \end{cases} \quad (13)$$

where x - y - z is right-handed ply coordinate system with x -axis representing the fibre direction. Y_t and Y_c are the *in situ* ply transverse tensile and compressive strengths respectively within the laminate and S_i is the *in situ* interlaminar shear strength. ${}^n \bar{\sigma}_y$ and ${}^n \bar{\tau}_{yz}$ are the averaged inplane transverse normal stress and averaged interlaminar transverse shear stress respectively within the n th ply. e_m is the strength ratio pertaining to matrix cracking. The region where e_m is greater than or equal to unity represents the location of the critical matrix cracking.

The semi-empirical delamination criterion for n th interface is given as (Choi and Chang 1992)

$$D_a \left[\left(\frac{\bar{\sigma}_y^{n+1}}{Y} \right)^2 + \left(\frac{\bar{\tau}_{yz}^n}{S_i} \right)^2 + \left(\frac{\bar{\tau}_{xz}^{n+1}}{S_i} \right)^2 \right] = e_d^2 \begin{cases} Y = Y_t, & \text{if } \bar{\sigma}_y \geq 0 \\ Y = Y_c, & \text{if } \bar{\sigma}_y < 0 \end{cases} \quad (14)$$

where D_a is an empirical constant, the value of which was suggested by Choi and Chang (1992). The subscript n and $n + 1$ correspond to the upper and lower plies of the n th interface respectively. $\bar{\tau}_{xz}^{n+1}$ is the averaged interlaminar longitudinal shear stress within the $(n+1)$ th ply. e_d is the strength ratio pertaining to delamination. The region, where e_d is greater than or equal to unity at the end of the impact, gives the estimation of the delamination size.

Although the above equations were proposed by Choi and Chang (1992) for the case of line-loading impact on laminated plate, several further investigators assumed this equation to be equally applicable to point-nose impact and also to curved shells. However as discussed earlier, Zhao and Cho (2004) have shown that damage propagation in shell takes place much differently from that in composite plate. Since the objective of this paper is mainly to demonstrate the effect of geometrical non-linearity, we here adopt the damage criteria suggested by Choi and Chang (1992) for damage analysis of cylindrical shells. Needless to mention here, any three-dimensional stress-based failure criteria can be implemented in the present formulation and the code.

3. Numerical results and discussions

The above non-linear finite element formulation was implemented in a specially developed computer code and some benchmark problems of isotropic and laminated composite problems were solved for validation.

Next, some example problems of T300/976 graphite/epoxy laminated cylindrical shell panels with variation of impactor parameters and shell dimensions and curvature are considered to study the impact behaviour of curved composite laminate. Effect of geometrical non-linearity on impact response and resulting damage are investigated. The problem descriptions of impact on a general

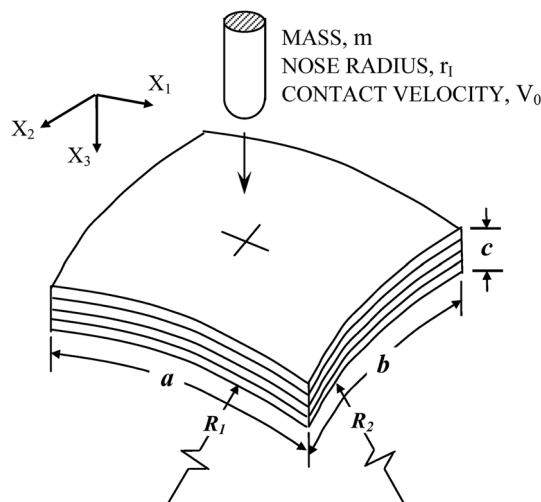


Fig. 2 Problem description of impact on a general doubly curved shell

doubly curved shell are depicted in Fig. 2 in which $x_1-x_2-x_3$ is the right-handed global (reference) coordinate system and the impacted side is the first layer in the stacking sequence. For all the example problems considered, the mesh size chosen is $12 \times 12 \times 4$ elements and mesh density is kept higher at the centre than the sides in the curvilinear plane of the laminate.

3.1 Validation

3.1.1 Large deformation of hinged-hinged and pinned-pinned beams

As an example, benchmark problem of simply-supported isotropic beam involving geometric nonlinearity is considered. A uniform beam of length $L = 100$, cross-section dimensions of 1×1 , made of a material with $E = 30 \times 10^6$ is considered. The beam is simply supported at both ends and subjected to a uniformly distributed load of intensity q per unit length. The units are consistently chosen, so that the exact deflection at the middle of the beam in linear bending theory is 0.5208, when $q = 1$. In linear bending theory, where the beam is assumed to undergo pure bending (i.e., there is no axial deformation); it is immaterial to consider whether the beam is allowed free movement in the axial direction at the supported ends. However, in non-bending, this is a crucial distinction. Hinged-hinged (HH) condition is designated for the case where there is no axial restraint at both ends and pinned-pinned (PP) condition for the one where there is full restraint. In the former case, inextensional bending occurs which is largely of a linear nature, and in the latter case, bending with extension exists. Both the cases are considered here. Using symmetry, half of the beam is modeled with $4 \times 1 \times 1$ elements and three different integration schemes i.e., standard $3 \times 3 \times 3$ (3 gauss points in all directions), $3 \times 3 \times 2$ (2 gauss points in thickness direction) and standard 14 points integration were employed.

The HH case is ideal to test the consistency aspect of the problem. As a non-linear element formulation is being used, a correct model should be able to recover the purely linear bending response under increasing load. This is possible only if the element can ensure that the inextensional axial condition (i.e., there is no axial restraint at both ends, no axial force should develop) is consistently recovered throughout. The PP case is ideal to examine the significance of the consistency aspect of the problem where the non-linear action becomes important. Table 1 shows the deflection under the load as q increases from 1 to 10. Results from Reddy (2004) are also shown in which two versions of beam element has been used. The first version which will have locking uses 2 points integration for bending energy and extensional energy while the second version which will be lock free uses 2 points integration for bending energy and 1 point integration for the extensional energy. It is clear that the present element model is able to capture both the behavior correctly.

3.1.2 Clamped 16-ply symmetric laminate subjected to uniform load

Next a 16-ply $[\pm 5/0_2/\mp 45/90_2]_S$ graphite-epoxy square laminate of size $b = 254$ mm and thickness $h = 2.114$ mm is considered. The plate is clamped on all edges and subject to uniform load q . The material properties of graphite-epoxy unidirectional ply are taken as:

$$E_{11} = 131 \text{ GPa}; E_{22} = E_{33} = 13.03 \text{ GPa}; G_{12} = G_{23} = G_{13} = 6.41 \text{ GPa}; \nu_{12} = \nu_{23} = \nu_{13} = 0.38.$$

Fig. 3 gives the comparison between present analysis and the results by Noor (1985) for laminate central deflection of the mid-ply. The present result is in good agreement with the results reported by the author.

Table 1 Central deflection for a simply supported beam under uniformly distributed load (UDL)

UDL per unit length, q	Present solution			Reddy (2004)	
	3×3×3 integration rule	3×3×2 integration rule	14 point integration rule	2×2 selective (energy-based) integration rule	2×1 selective (energy-based) integration rule
(A) Hinged-Hinged (HH) Condition					
1	0.514751	0.514751	0.513443	0.5108	0.5208
2	1.02881	1.02881	1.02620	0.9739	1.0417
3	1.54128	1.54128	1.53738	1.3764	1.5625
4	2.05131	2.05131	2.04612	1.7265	2.0833
5	2.55805	2.55806	2.55161	2.0351	2.6042
6	3.06073	3.06073	3.05304	2.3116	3.1250
7	3.55859	3.55859	3.54970	2.5630	3.6458
8	4.05098	4.05098	4.04091	2.7930	4.1667
9	4.53727	4.53727	4.52606	3.0060	4.6875
10	5.01692	5.01692	5.00460	3.2051	5.2083
(B) Pinned-Pinned (PP) Condition					
1	0.366698	0.366698	0.366272	0.3669	0.3687
2	0.544018	0.544018	0.543636	0.5424	0.5466
3	0.662900	0.662900	0.662555	0.6601	0.6663
4	0.754704	0.754704	0.754387	0.7510	0.7591
5	0.830619	0.830620	0.830323	0.8263	0.8361
6	0.895961	0.895961	0.895682	0.8912	0.9027
7	0.953697	0.953698	0.953432	0.9485	0.9617
8	1.00567	1.00567	1.00541	1.0002	1.0150
9	1.05309	1.05309	1.05285	1.0473	1.0638
10	1.09683	1.09683	1.09660	1.0908	1.1089

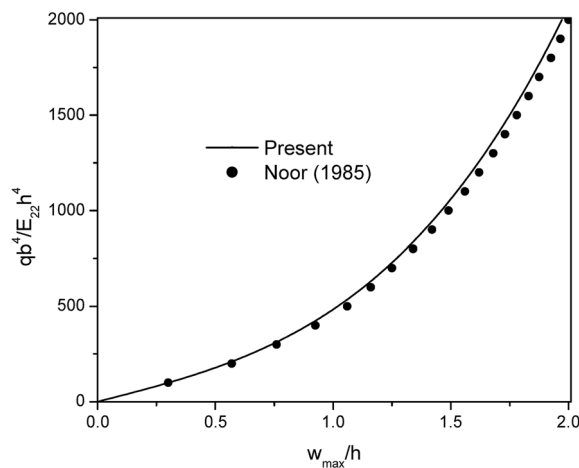


Fig. 3 Load-deflection curve for 16-ply $[\pm 5/0_2/\mp 45^\circ/90_2]_S$ square laminate (size $b=254$ mm and thickness $h=2.114$ mm) with clamped edges and subjected to uniform load

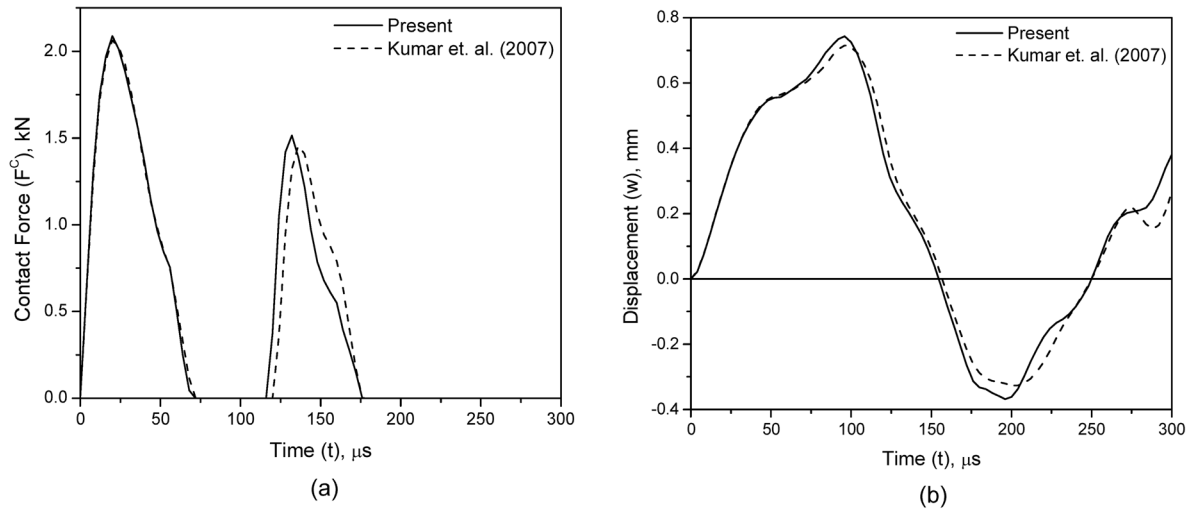


Fig. 4 Comparison of (a) contact force and (b) plate centre displacement in a 76.2 by 76.2 mm T300/934 graphite/epoxy laminated plate $[0/-45/45/90]_{2S}$ with clamped edges impacted by 12.7 mm diameter aluminum sphere at a velocity of 25.4 ms^{-1}

3.1.3 Impact response of a rectangular graphite/epoxy laminated plate

As another example, a rectangular graphite/epoxy laminated plate with a ply orientation of $[0/-45/45/90]_{2S}$ is investigated with plate dimensions and impactor parameters to be same as those taken in an earlier paper by the author (Kumar *et al.* 2007). A linear analysis was carried out for this problem and the results of contact force and plate centre displacement are presented in Fig. 4 along with the literature results (Kumar *et al.* 2007) obtained by linear analysis using eight noded layered brick element. A good agreement between the two results may be observed.

3.2 Impact response

T300/976 Graphite/epoxy cylindrical shells of different dimensions and curvatures with $[90_4/0_8/90_4]$ lay-up and clamped on their edges are considered. At first, $[90_4/0_8/90_4]$ cylindrical shell is taken with geometric properties: $a=b=100 \text{ mm}$; $R_1=R=10a$, a ; and $R_2=\infty$ (Fig. 2). The impactor is a steel mass of 200 gm having a half sphere head of 10 mm diameter and initial velocity 5 ms^{-1} . The material properties of fiberite T300/976 graphite/epoxy composite are considered as listed in reference (Choi and Chang 1992). The results of contact force, impactor displacement and shell centre displacement are presented in Fig. 5 for linear and non-linear analyses of shell curvatures $R=10a$ and $R=a$. The maximum contact force increases and both contact duration and amplitude of shell response decrease with decrease in shell radius. This signifies that increasing the curvature has a stiffening effect on the cylindrical shell which increases the natural frequencies. For the shell with curvature $R=a$, a considerable reduction in peak contact force and increase in both contact period as well as maximum shell central deflection were observed, when non-linearity was implemented in the analysis. However, these differences were not significant in case of shell with curvature $R=10a$ despite this shell having more central deflection. Instead, a small increase in peak contact force and a marginal decrease in contact period and maximum central deflection were observed. This indicates

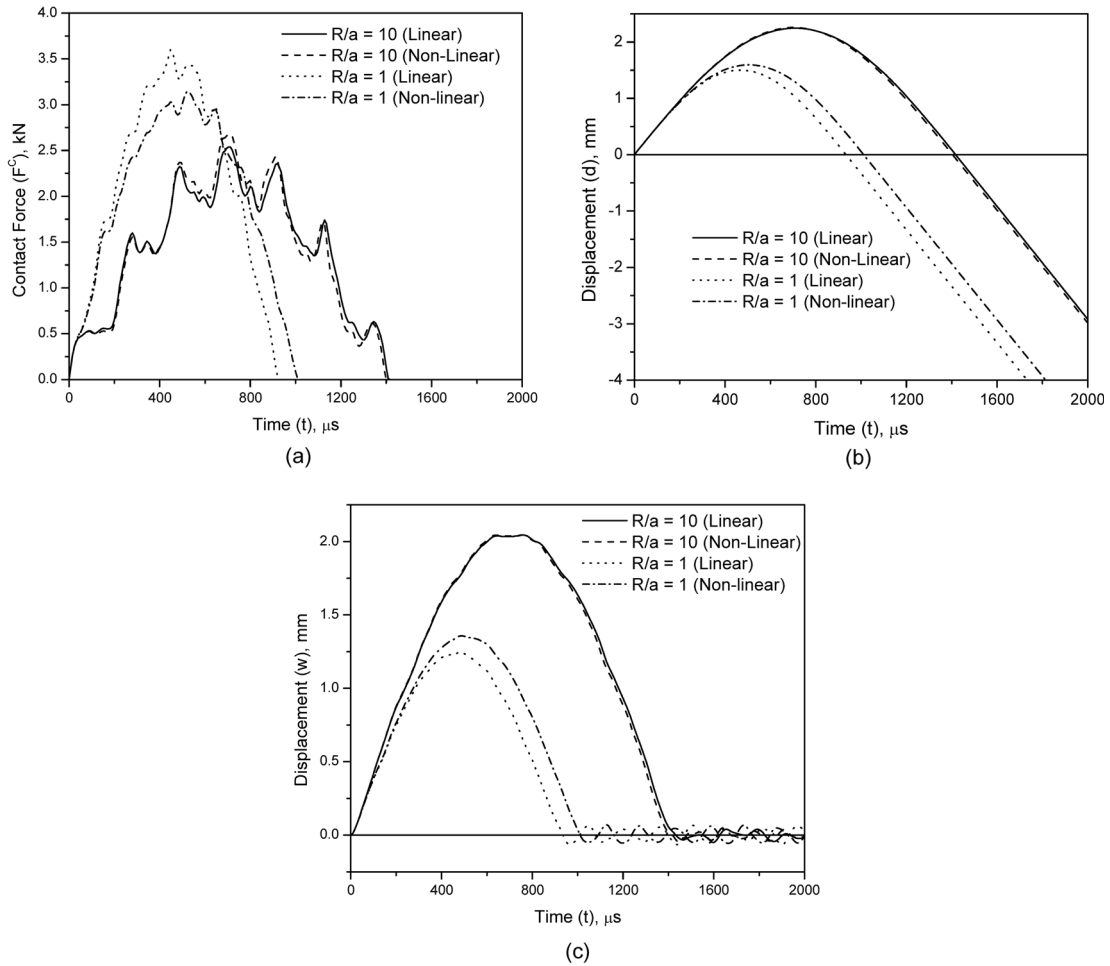


Fig. 5 (a) Contact force, (b) impactor displacement and (c) plate centre displacement in graphite/epoxy cylindrical shells ($[90_4/0_8/90_4]$) ($a=b=100$ mm; $R=10a$ and $R=a$), with clamped edges and impacted by blunt-ended steel cylinder of nose radius 5 mm and mass 200 gm having initial velocity of 5 ms^{-1}

that non-linear approach has caused decrease in flexural rigidity of the shell having higher stiffness due to curvature while this has resulted in increase in flexural rigidity of the shell having lower curvature-induced stiffness.

Next, cylindrical shell of larger dimensions $a=b=300$ mm and curvature $R=a$ is considered which is again clamped on its edges and is subjected to impact by a steel mass of 200 gm having a half sphere head of 10 mm diameter and initial velocity 10 ms^{-1} . The results of contact force, impactor displacement and shell centre displacement are plotted in Fig. 6 for linear and non-linear solutions. Again a noticeable increase in contact duration and small reduction in maximum contact force are observed in case of non-linear approach. Maximum central deflection also increased considerably in non-linear solution. A comparison of this result with that of Fig. 5 leads to the conclusion that effect of geometrical non-linearity is more pronounced in the problem case of Fig. 6. This can be attributed to the reason that maximum shell deflection in the problem of Fig. 6 is

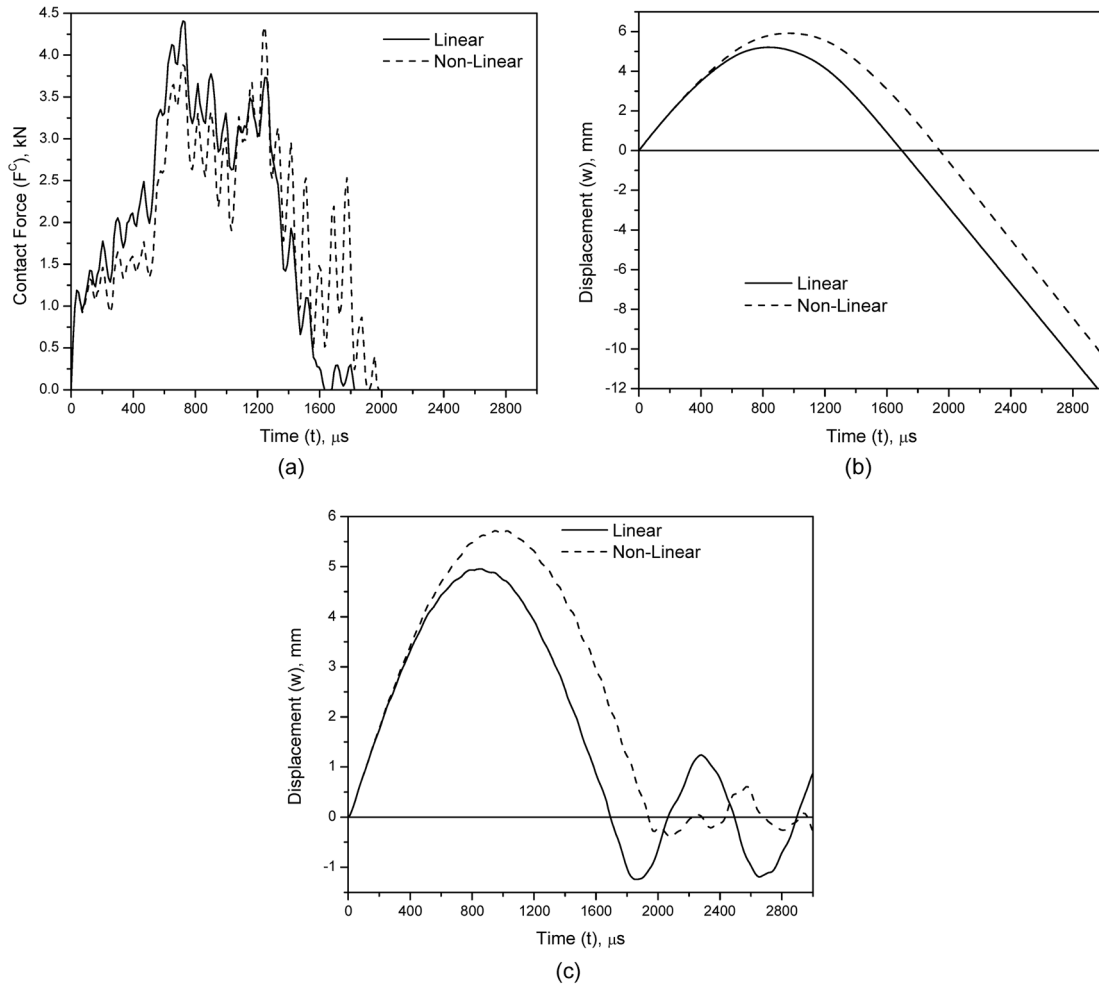


Fig. 6 (a) Contact force, (b) impactor displacement and (c) centre displacement in graphite/epoxy cylindrical shell ($[90_4/0_8/90_4]$ lay-up) ($a=b=300$ mm; $R=a$), with clamped edges and impacted by blunt-ended steel cylinder of nose radius 5 mm and mass 200 gm having initial velocity of 10 ms^{-1}

significantly more than that in the problem of Fig. 5 and even higher than the shell thickness.

3.3 Impact-induced damages

Impact-induced damages (critical matrix cracking and the extent of delamination) are studied for the above cylindrical shells. The shell with $[90_4/0_8/90_4]$ lay-up with dimensions $a=b=100$ mm and curvatures $R=10a$ and $R=a$ is subjected to impact by a steel mass of 200 gm and nose radius 5 mm traveling at a velocity of 5 ms^{-1} . The value of strength ratio, e_m (critical matrix cracking failure criterion) at any point in the bottom $[90_4]$ ply group of the shell is found to be maximum at time approximately 720 μs for $R/a=10$ (linear analysis), 712 μs for $R/a=10$ (non-linear analysis), 440 μs for $R/a=1$ (linear analysis) and at 520 μs for $R/a=1$ (non-linear analysis), as plotted in isometric view in Fig. 7. The matrix cracking failure contour is extended much wider along the

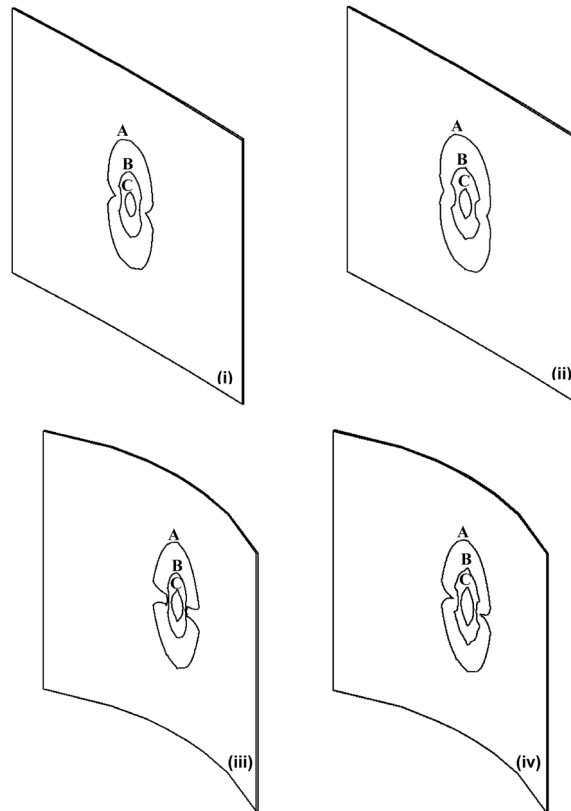


Fig. 7. Maximum strength ratio, e_m in bottom $[90_4]$ ply of $[90_4/0_8/90_4]$ cylindrical shells (dimensions: $a=b=100$ mm) having different curvatures (i) $R/a=10$ (linear analysis), (ii) $R/a=10$ (non-linear analysis), (iii) $R/a=1$ (linear analysis) and (iv) $R/a=1$ (non-linear analysis), all with clamped edges and impacted by 200 gm mass at a velocity of 5 ms^{-1} (e_m values: A=0.2, B=0.5, C=1.0)

fibre direction of the cracked $[90_4]$ ply group than in the direction normal to the fibre direction.

The maximum values of strength ratio, e_d (impact-induced delamination criterion) in the bottom 0/90 plies interface during the impact are plotted in Fig. 8 for the four cases. It is seen that delamination propagates much wider in the fibre direction of the $[90_4]$ ply group below the delaminated interface than in the direction normal to it.

From Figs. 7 and 8, it is observed that there is a considerable increase in the sizes of both the damages in case of non-linear solutions for the shell with higher curvature ($R=a$) despite the fact that maximum contact force was less in non-linear case. This increase in damage size can be mainly attributed to larger shell deflection and hence larger bending stress attributing to matrix cracking and delamination. In case of shell with lower curvature ($R=10a$) also, there is a considerable difference in the damage profiles obtained by linear and non-linear solutions.

Impact-induced damages are also predicted for the example problem of Fig. 6. The value of strength ratio, e_m at any point in the shell with $[90_4/0_8/90_4]$ lay-up is found to be maximum in the bottom $[90_4]$ ply group at time approximately $660 \mu\text{s}$ in case of linear solution and $1164 \mu\text{s}$ in case of non-linear solution, as plotted in Fig. 9. The maximum value of strength ratio, e_d and predicted delamination size in the bottom 0/90 plies interface of $[90_4/0_8/90_4]$ lay-up are plotted in Fig. 10 for

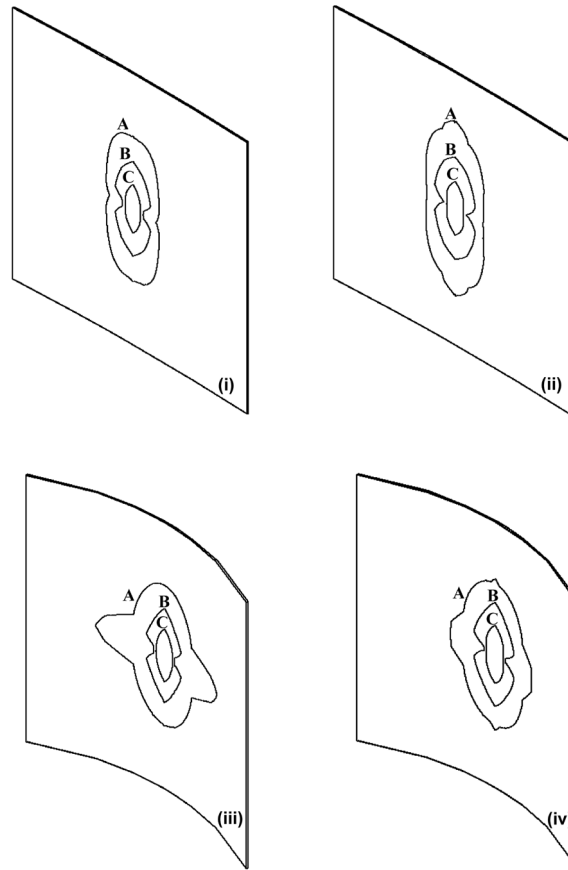


Fig. 8 Maximum strength ratio, e_d and predicted delamination sizes at 0/90 interface of $[90_4/0_8/90_4]$ cylindrical shells (dimensions: $a=b=100$ mm) having different curvatures (i) $R/a=10$ (linear analysis), (ii) $R/a=10$ (non-linear analysis), (iii) $R/a=1$ (linear analysis) and (iv) $R/a=1$ (non-linear analysis), all with clamped edges and impacted by 200 gm mass at a velocity of 5 ms^{-1} (e_d values: A=0.2, B=0.5, C=1.0)

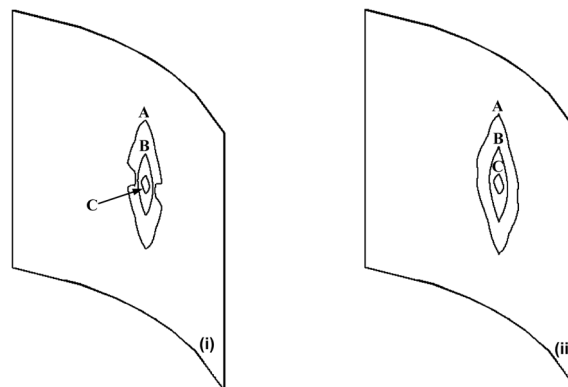


Fig. 9 Maximum strength ratio, e_m in bottom $[90_4]$ ply of $[90_4/0_8/90_4]$ lay-up cylindrical shell (dimensions: $a=b=300$ mm; $R=a$) with clamped edges and impacted by 200 gm mass at a velocity of 10 ms^{-1} : (i) linear analysis and (ii) non-linear analysis (e_m values: A=0.2, B=0.5, C=1.0)

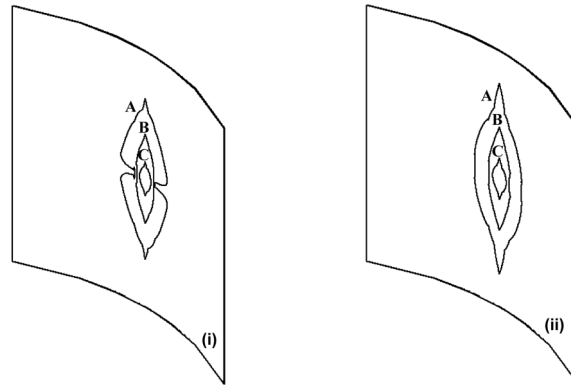


Fig. 10 Maximum strength ratio, e_d and predicted delamination sizes at 0/90 interface of $[90_4/0_8/90_4]$ lay-up cylindrical shell (dimensions: $a=b=300$ mm; $R=a$) with clamped edges and impacted by 200 gm mass at a velocity of 10 ms $^{-1}$: (i) linear analysis and (ii) non-linear analysis (e_d values: A=0.2, B=0.5, C=1.0)

the two cases. Again there is a considerable increase in size and change in profile of damages in non-linear case when compared with those in linear case.

4. Conclusions

Three-dimensional non-linear finite element and transient dynamic analysis of laminated composite cylindrical shell panel subjected to transverse impact is performed using 20 noded layered hexahedral element and implemented by a specially developed computer code. The tangent stiffness matrix accounting for the geometric non-linearity is formulated using generalized Green's strain tensor. The non-linear system of equations was solved iteratively using Newton-Raphson method by considering suitable displacement and force convergence norms. Several numerical problems of graphite/epoxy laminated cylindrical shells are studied with variation of parameters such as impactor mass and velocity, shell dimension and shell curvature. The major focus has been given to investigate non-linear geometrical effects on impact response and resulting damages. Some specific observations can be deduced from the study:

- (1) When geometrical non-linearity was considered, considerable changes in time-variations of contact force, impactor displacement and shell deflection were observed. However, the effect of non-linearity was observed to be significantly different for different curvatures, indicating that there exists coupling between flexibility brought by geometrical non-linearity and curvature-induced stiffness.
- (2) The effect of geometrical non-linearity on impact response was found to be more pronounced for the cases when the shell deflection is higher than the shell thickness.
- (3) Considerable changes in the sizes and profiles of both the impact damages (critical matrix cracking and delamination) are noticed when a non-linear approach is used in the solution. Since the damages were calculated at the bottommost ply of the laminate, the difference in damage profiles predicted by linear and non-linear solutions was quite consistent with the difference in shell deflections and not the contact forces.

References

- Abrate, S. (1994), "Impact on laminated composites: recent advances", *Appl. Mech. Rev.*, **47**, 517-544.
- Ambur, D.R., Starnes, J.H. Jr. and Prasad, C.B. (1995), "Low-speed impact damage initiation characteristics of selected laminate composite plate", *AIAA J.*, **33**, 1919-1925.
- Chandrashekhara, K. and Schroeder, T. (1995), "Nonlinear impact analysis of laminated cylindrical and doubly curved shells", *J. Compos. Mater.*, **29**(16), 2160-2179.
- Cho, C. and Zhao, G. (2002), "Effects of geometric and material factors on mechanical response of laminated composites due to low velocity impact", *J. Compos. Mater.*, **36**(12), 1403-1428.
- Choi, H.Y. and Chang, F.K. (1992), "A model for predicting damage in graphite/epoxy laminated composites from low-velocity point impact", *J. Compos. Mater.*, **26**, 2134-2169.
- Ganapathy, S. and Rao, K.P. (1998), "Failure analysis of laminated composite cylindrical/spherical shell panels subjected to low-velocity impact", *Comput. Struct.*, **68**, 627-641.
- Gning, P.B., Tarfaoui, M., Collombet, F. and Davies, P. (2005), "Prediction of damage in composite cylinders after impact", *J. Compos. Mater.*, **39**(10), 917-928.
- Her, S.C. and Liang, Y.C. (2004), "The finite element analysis of composite laminates and shell structures subjected to low velocity impact", *Comput. Struct.*, **66**, 277-285.
- Hou, J.P., Petrinic, N., Ruiz, C. and Hallet, S.R. (2000), "Prediction of impact damage in composite plates", *Compos. Sci. Technol.*, **60**(2), 273-281.
- Hou, J.P., Petrinic, N. and Ruiz, C. (2001), "A delamination criterion for laminated composites under low-velocity impact", *Compos. Sci. Technol.*, **61**(14), 2069-2074.
- Krishnamurthy, K.S., Mahajan, P. and Mittal, R.K. (2001), "A parametric study of the impact response and damage of laminated cylindrical composite shells", *Compos. Sci. Technol.*, **61**(12), 1655-1669.
- Krishnamurthy, K.S., Mahajan, P. and Mittal, R.K. (2003), "Impact response and damage in laminated composite cylindrical shells", *Comput. Struct.*, **59**, 15-36.
- Kumar, S., Rao, B.N. and Pradhan, B. (2007), "Effect of impactor parameters and laminate characteristics on impact response and damage in curved composite laminates", *J. Reinf. Plast. Comp.*, **26**(13), 1273-1290.
- Noor, A.K. (1985), "Hybrid analytical technique for nonlinear analysis of structures", *AIAA J.*, **23**(6), 938-946.
- Reddy, J.N. (2004), *An introduction to Non-linear Finite Element Analysis*, Oxford University Press, Oxford.
- Yang, S.H. and Sun, C.T. (1982), "Indentation law for composite laminates", *Composite Materials: Testing & Design (6th Conference)*, American Special Technical Publication, 425-449.
- Zhao, G. and Cho, C. (2004), "On impact damage of composite shells by a low-velocity projectile", *J. Compos. Mater.*, **38**(14), 1231-1254.
- Zhu, L., Chattopadhyay, A. and Goldberg, R.K. (2006), "Multiscale analysis including strain rate dependency for transient response of composite laminated shells", *J. Reinf. Plast. Comp.*, **25**(17), 1795-1831.
- Zienkiewicz, O.C. and Taylor, R.L. (1993), *The Finite Element Method*, McGraw-Hill, NY.